Available online at www.sciencedirect.com
ScienceDirect
Journal of Hazardous Materials 150 (2008) 737–746
Journal of Hazardous Materials
www.elsevier.com/locate/jhazmat

Adsorption of reactive dyes from aqueous solutions by fly ash: Kinetic and equilibrium studies

N. Dizge [a], C. Aydiner [a], E. Demirbas [b,*], M. Kobya [a], S. Kara [a]

[a] *Gebze Institute of Technology, Department of Environmental Engineering, 41400 Gebze, Turkey*
[b] *Gebze Institute of Technology, Department of Chemistry, 41400 Gebze, Turkey*

Received 4 April 2006; received in revised form 27 April 2007; accepted 9 May 2007
Available online 13 May 2007

Abstract

Adsorption kinetic and equilibrium studies of three reactive dyes namely, Remazol Brillant Blue (RB), Remazol Red 133 (RR) and Rifacion Yellow HED (RY) from aqueous solutions at various initial dye concentration (100–500 mg/l), pH (2–8), particle size (45–112.5 μm) and temperature (293–323 K) on fly ash (FA) were studied in a batch mode operation. The adsorbent was characterized with using several methods such as SEM, XRD and FTIR. Adsorption of RB reactive dye was found to be pH dependent but both RR and RY reactive dyes were not. The result showed that the amount adsorbed of the reactive dyes increased with increasing initial dye concentration and contact time. Batch kinetic data from experimental investigations on the removal of reactive dyes from aqueous solutions using FA have been well described by external mass transfer and intraparticle diffusion models. It was found that external mass transfer and intraparticle diffusion had rate limiting affects on the removal process. This was attributed to the relatively simple macropore structure of FA particles. The adsorption data fitted well with Langmuir and Freundlich isotherm models. The optimum conditions for removal of the reactive dyes were 100 mg/l initial dye concentration, 0.6 g/100 ml adsorbent dose, temperature of 293 K, 45 μm particle size, pH 6 and agitation speed of 250 rpm, respectively. The values of Langmuir and Freundlich constants were found to increase with increasing temperature in the range 135–180 and 15–34 mg/g for RB, 47–86 and 1.9–3.7 mg/g for RR and 37–61 and 3.0–3.6 mg/g for RY reactive dyes, respectively. Different thermodynamic parameters viz., changes in standard free energy, enthalpy and entropy were evaluated and it was found that the reaction was spontaneous and endothermic in nature.

Keywords: Reactive dyes; Fly ash; Adsorption isotherms; External diffusion; Intraparticle diffusion

1. Introduction

In textile dyeing processes, a large volume of dye-contaminated effluent is discharged, and it was estimated that 10–15% of the dye is lost in the dye effluent. The effluents of these industries are highly colored and the disposal of these wastes into receiving waters causes damage to the environment as they may significantly affect photosynthetic activity in aquatic life due to reduced light penetration and may also be toxic to some aquatic life due to the presence of metals, chlorides, etc., in them [1].

Reactive dyes are typically azo-based chromophores combined with different types of reactive groups. They differ from all other classes of dyes in that they bind to the textile fibers such as cotton to form covalent bonds. They have the favorable characteristics of bright color, simple application techniques and low energy consumption and are used extensively in textile industries. Hence their removal is also of great importance [2].

There are a number of methods for dye removals which include chemical coagulation, flocculation, chemical oxidation, photochemical degradation, membrane filtration, including aerobic and anaerobic biological degradation but all of these methods suffer from one or other limitations, and none of them were successful in completely removing the color from wastewater. Dyes can be effectively removed by adsorption process; in which dissolved dye compounds attach themselves to the surface of adsorbents [3,4]. Adsorption has been extensively used in industrial processes for either separation or purification. Most conventional adsorption plants use activated carbon, which is an expensive material. Besides, there is growing interest in searching for cheaper sources as low-cost adsorbent materials for the

* Corresponding author. Tel.: +90 262 6053108; fax: +90 262 6053101.
E-mail address: erhan@gyte.edu.tr (E. Demirbas).

0304-3894/$ – see front matter © 2007 Elsevier B.V. All rights reserved.
doi:10.1016/j.jhazmat.2007.05.027

Nomenclature

A	total interfacial area of the particles (cm^2)
b	energy of adsorption (l/mg)
B_N	Biot number
C_0	initial liquid-phase concentration (mg/l)
C_t	initial liquid-phase concentration at time (mg/l)
C_e	equilibrium liquid-phase concentration (mg/l)
d	mean particle diameter (μm)
D	sum of pore and surface diffusion (cm^2/s)
K_c	equilibrium constant of the adsorption process
k_f	initial external mass transfer coefficient (cm/s)
k_F	Freundlich isotherm constant (mg/g)
k_{id}	intraparticle diffusion rate constant (mg/g $min^{1/2}$)
m	adsorbent dosage (g/cm^3)
q_e	solute concentration retained in the adsorbent phase (mg/g)
q_t	solid concentration retained in the adsorbent phase at time (mg/g)
Q_0	adsorption capacity (mg/g)
R	gas constant (J/mol K)
RB	Remazol Blue
RR	Remazol Red
RY	Rifacion Yellow
t	time (min)
T	temperature (K)
V	volume of solution (l)
W_s	mass of the adsorbent (g)
ΔG°	free energy change (kJ/mol)
ΔH°	entalpy change (kJ/mol)
ΔS°	entropy change (kJ/K mol)
ρ	apparent density of the adsorbent (g/cm^3)

adsorption of dyes such as coir pith, sugar cane dust, sawdust, activated carbon fibers [5–9], industrial solid wastes: fly ash, shale oil ash, and so on [10–15].

During coal-fired electric power generation, two main types of coal combustion by-products are obtained, fly ash (FA) and bottom ash. The current annual worldwide production of coal ash is estimated about 700 million tones of which at least 70% is FA [16]. Although, significant quantities are being used in a range of applications and particularly as a substitute for cement in concrete, large amounts are not used and this requires disposal. Making a more productive use of FA would have considerable environmental benefits, reducing air and water pollution. About 55 million tons of coal and lignite is combusted annually in Turkey resulting in more than 15 million tones of FA.

In the present study, the adsorption ability of three reactive commercial dyes, Remazol Brillant Blue (RB), Remazol Red 133 (RR) and Rifacion Yellow HED (RY) using FA as an adsorbent from aqueous solutions was examined. Effects of initial dye concentration, pH, particle size and temperature on FA under kinetic and equilibrium conditions were investigated. The rate limiting step of three reactive dye adsorptions onto FA is determined from the adsorption kinetic results. Both Langmuir and Freundlich adsorption isotherms were applied to the experimental results and thermodynamic parameters were also calculated.

2. Materials and methods

2.1. Materials

The FA was obtained from Afsin-Elbistan Thermal Power Station in Turkey. The Afsin-Elbistan power plant consumes 18×10^6 metric tones of coal per year and generates about 3.24×10^6 metric tones of FA returning to the dumping area of the mine as combustion waste. The particle size distribution of FA was found between 3.6 and 181 μm. Higher percentage of FA consists of particles with diameter 40–125 μm (determined by the method of laser beam dispersion using the Malvern 2000 particle size analyzer). FA was sieved by using a sieve set and then was collected in the range of 40–50, 63–80 and 100–125 μm, respectively. The surface area of the FA was measured by BET (Brunauer–Emmett–Teller nitrogen adsorption technique). The bulk density of the adsorbent was determined with a densitometer. FA was used as received without any pretreatment in the adsorption experiments.

Three reactive dyes obtained from Dystar and Itochu were used in the adsorption study. Their chemical structures and characterizations are displayed in Fig. 1 and Table 1, respectively.

2.2. Methods

The study of adsorption kinetics and equilibrium is essential in supplying the fundamental information required for the design and operation of adsorption equipments for wastewater treatment. The effect of experimental parameters such as, pH (2–8), initial dye concentration (100–500 mg/l), particle size (45–112.5 μm) and temperature (293–323 K) on the adsorptive removal of reactive dyes on FA was investigated in batch experiments. The minimum amount of FA corresponding to the maximum adsorption is declared as the optimum dosage. The optimum dose observed in the present study is 0.6 g/100 ml. For each experimental run, 50 ml of dye solution of known concentration, pH and known amount of the adsorbent were taken in a 250 ml conical flask. The mixture was agitated in a temperature controlled shaker at a constant speed of 250 rpm for 24 h at a constant temperature of 293 K. At predecided intervals the solutions of the specified flask were separated from the adsorbent materials and concentration of dye was determined spectrophotometrically on a Perkin-Elmer UV–visible spectrophotometer model 550S by measuring absorbance at a wavelength of 518, 585 and 411 nm for RR, RB and RY reactive dyes, respectively. The pH of the dye solution was adjusted by 0.1N NaOH or 0.1N HCl. Kinetics of adsorption was determined by analyzing adsorptive uptake of the dye from aqueous solution at different time intervals. For adsorption isotherms, dye solutions of different concentrations were agitated with known amount of adsorbent at fixed pH, agitation speed and particle size till the equilibrium was reached (48 h). The concentration retained in the adsorbent phase (q_e, mg/g) was calculated by using the

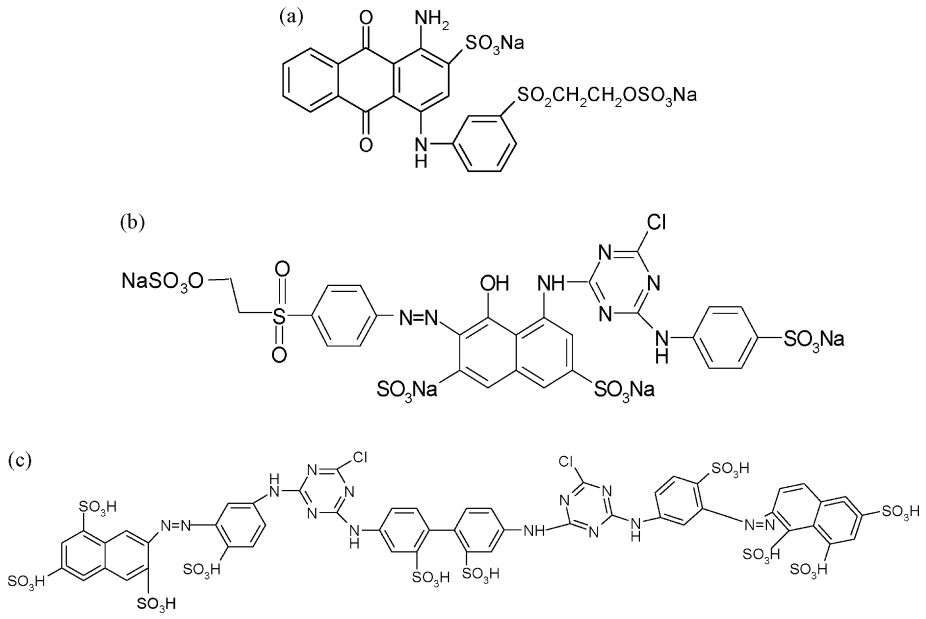

Fig. 1. Chemical structure of the reactive dyes (a) Remazol Brillant Blue (RB), (b) Remazol Red 133 (RR) and (c) Rifacion Yellow HED (RY).

Table 1
Characterizations of RB, RR and RY reactive dyes

Parameters	Remazol Brillant Blue (RB)	Remazol Red 133 (RR)	Rifacion Yellow HED (RY)
Color index name	Reactive Blue 19	Reactive Red 198	Reactive Yellow 84
Chromophore group	Anthraquinone	Azo	Disazo
Reactive anchor systems[a]	VS	MCT + VS	ACT
Molar mass (g/mol)	506.5	984.2	1922
Max absorbance, λ_m (nm)	585	518	411
Purity (%)	∼50	∼63	∼80
Water solubility at 293 K (g/l)	100	70	70
Acute oral toxicity LD_{50} (mg/kg)	2000	2000	–
Fish toxicity LC_0 (mg/l)	–	>500	–
pH value (10 g/l water)	5–5.5	7	6.5
COD (mg/g)	–	540	160
BOI_5 (mg/g)	–	<10	–
DOC (mg/g)	–	120	–
Company	Dystar	Dystar	Itochu

[a] Monochlortriazine (MCT); Bisaminochlorotriazine (ACT); vinylsulfone (VS).

following equation:

$$q_e = \frac{(C_0 - C_t)V}{W_s} \quad (1)$$

where C_0 is the initial dye concentration and C_t is the dye concentration (mg/l) at any time, V the volume of solution (l) and W_s is the mass of the adsorbent (g). Each experiment was carried out in duplicate and the average results are presented.

3. Diffusion controlled kinetic models

Mass transfer within FA particles can be complex since adsorption is inherently a transient process involving some sort of Fickian diffusion in both the fluid and adsorbed phases. An understanding of significance of diffusional mechanisms and accurate estimates of the diffusivities inside the adsorbent particles are determined from the diffusion controlled kinetic models based on interpretation of the experimental data. The external diffusion model [17,18] assumes that the concentration at the adsorbent surface tends to zero and the intraparticle diffusion is negligible at early times of contact. External diffusion is described in the following equation:

$$\ln \frac{C_t}{C_0} = -k_f \frac{A}{V} t \quad (2)$$

where C_0, C_t, A/V and t are the initial ion concentration, concentration at time, the total interfacial area of the particles (cm^2) to the total solution volume (l) and adsorption time, respectively. A/V is expressed as

$$\frac{A}{V} = \frac{3m}{\rho d} \quad (3)$$

where m is the adsorbent dosage (g/cm^3), d the mean particle diameter (μm), and ρ is the apparent density of the adsorbent

(g/cm^3). By plotting $\ln(C_t/C_0)$ against t, the initial external mass transfer coefficient, k_f (cm/s) may be determined.

The mathematical relationship between the concentration of adsorbed substance onto the solid surface and $t^{1/2}$ has been deduced by considering the adsorption mechanism being controlled by intraparticle diffusion in the adsorbent [19]

$$q_t = k_{id} t^{1/2} + C \tag{4}$$

where k_{id} is the intraparticle diffusion rate constant (mg/g min$^{1/2}$). According to Eq. (4), a plot of q_t versus $t^{1/2}$ should be a straight line with a slope k_{id} and intercept C when adsorption mechanism follows the intraparticular diffusion process. Values of the intercept give an idea about the thickness of boundary layer, i.e., the larger the intercept is the greater the boundary layer effect.

Pore and surface mass diffusion is governed by Fick's law and intraparticle diffusion, D, the sum of pore and surface diffusion, may simply be calculated from the following equation [20]:

$$-\log\left(1-\left(\frac{q_t}{q_e}\right)^2\right) = \left(\frac{4\pi^2 D}{2.3d^2}\right) t \tag{5}$$

where q_t and q_e are the solute concentration in the solid at time t and at equilibrium. Once the external and internal diffusion coefficients are determined for a given adsorption system, the Biot number can then be estimated from the following equation:

$$B_N = k_f \frac{d}{D} \tag{6}$$

The Biot number gives a criterion for the predominance of surface diffusion against external diffusion. Adsorption processes are mainly controlled by internal diffusion mechanisms where the Biot number is greater than 100 [21].

4. Results and discussion

4.1. Characterization of the adsorbent material

Chemical composition of FA as determined by chemical analysis is SiO_2, 15.14; Fe_2O_3, 3.30; Al_2O_3, 7.54; CaO, 23.66; MgO, 4.5; SO_3, 13.22; K_2O, 0.28; Na_2O, 0.57 and TiO_2, 1.03 and lost on ignition, 2.31 wt%. The specific surface area, bulk density, specific gravity and moisture content of FA are determined as 0.342 m^2/g, 1.05 g/cm^3, 2.70 g/cm^3 and 3%, respectively [22]. The zero point charge (ZPC) for FA is found to be 7.0 [13]. The surface of adsorbent was characterized by scanning electron microscopy (SEM, Philips XL30S-FEG) before and after the adsorption experiments using RR dye (Fig. 2). The SEM image clearly shows that FA particles are mainly composed of irregular and porous particles.

4.2. XRD measurements

The XRD for the adsorbent was measured with an automated Rigaku X-ray diffractometer D-Max Rint 2200 Series instrument using Cu Kα radiation at 40 kV and 40 mA over the range (2θ of 5–70°). The XRD pattern for FA is shown in Fig. 3. It is seen that there are not much significant difference for XRD profiles. But RR dye-loaded FA sample present higher intensity of diffraction peaks. Differences in the XRD patterns are caused by the lowering in crystallinity of the FA during the sorption. The major phases for the sample are quartz, mullite with some magnetite and calcite. The result suggests that the dye-loaded FA will not induce bulk phase changes.

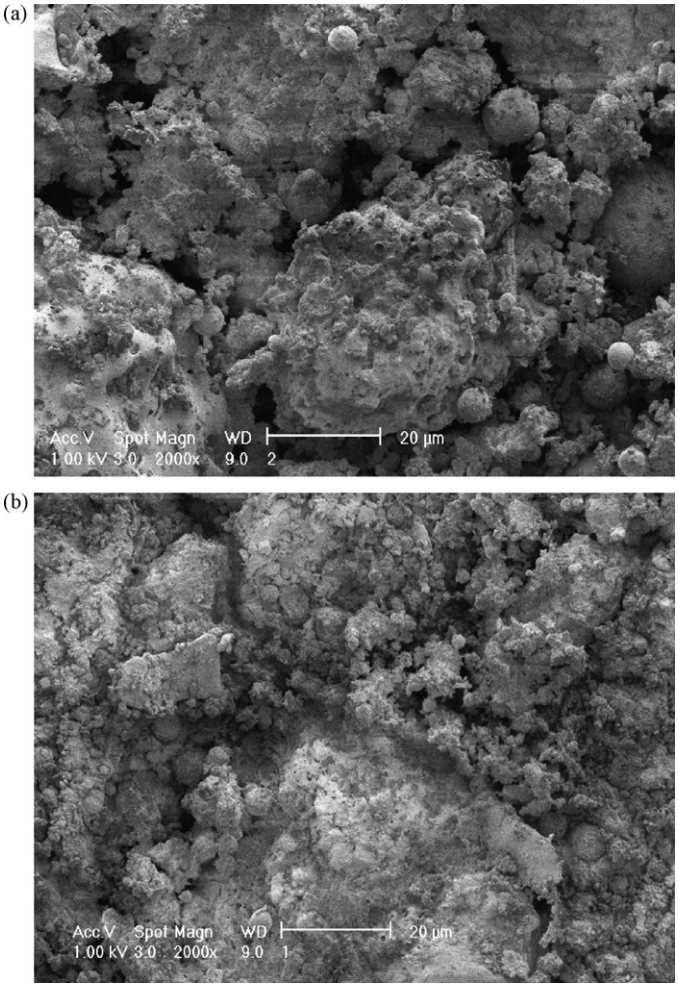

Fig. 2. Typical SEM micrograph of FA (magnification: 2000×) (a) before dye adsorption and (b) with dye adsorbed.

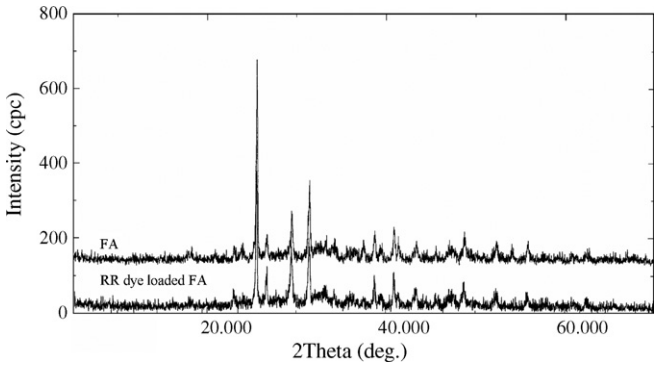

Fig. 3. XRD patterns of (a) FA and (b) RR dye-loaded FA.

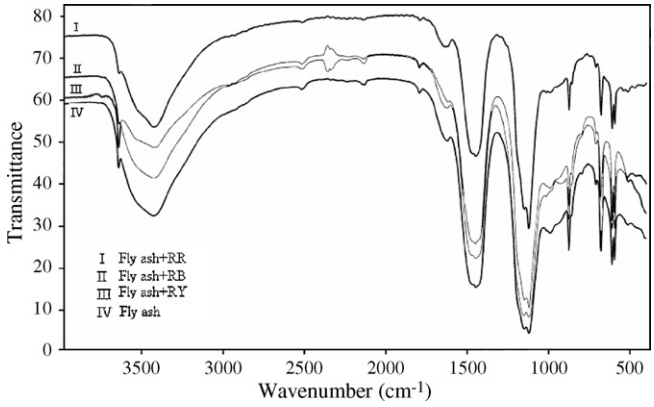

Fig. 4. FTIR spectra of FA and dye-loaded FA samples.

4.3. FTIR measurements

FTIR technique was used to examine the surface groups responsible for dye adsorption. FA and dye-loaded FA samples after adsorption were placed in a oven at 80 °C for 6 h. Samples were made as pellet and then the infrared spectra of three dyes on FA before and after the adsorption process were recorded in the range 4000–400 cm^{-1} on a Bio Rad FTS 175 C spectrophotometer (Fig. 4). The adsorption bands at 595.5–1637.8 cm^{-1} were assigned to SO_3 and –N=N– groups on the samples. The strong bands at 993.3, 1120.9 and 1149.4 cm^{-1} regions are attributed to S=O stretching and the bands at 1626–1637.8 cm^{-1} attributed to –N=N– stretching, diminished after adsorption. Furthermore, the bands at 1450 and 1627 cm^{-1} assigned to aromatic skeletal vibrations have been shifted, broadened and reduced after adsorption. Strong Si–O bands at 875–1121 cm^{-1} are shifted to higher frequencies as a function of chemical interaction of the dyes with FA. The stretching adsorption band of O–H in the crystal structure of the adsorbent is observed at 3645 cm^{-1} assigned to free hydroxyl and diminished after adsorption with the reactive dye. All these findings suggest the attachment of dyes on the FA [13,23].

4.4. Effect of pH on adsorption kinetics

The variation of adsorption of three reactive dyes by FA over a broad pH range (2–8) at an initial dye concentration of 100 mg/l, a temperature of 293 K and agitation speed of 250 rpm is shown in Fig. 5. The amount adsorbed increased from 11 to 44 mg/g for RB, from 23 to 49 mg/g for RR and from 23 to 43 mg/g for RY reactive dyes, respectively, as the pH increased from 2 to 8. Adsorption of RB reactive dye was found to be pH dependent to some extent but the adsorption capacity of FA for both RR and RY reactive dyes was not affected significantly with changes of pH. pH of the dye solution without pH being adjusted is 6 and there is also not much difference between values of the adsorbent capacities for three reactive dyes. pH 6.0 is selected in the subsequent experiments since surface charge of FA is positive below the pHpzc, i.e., 7.0 which maximizes the adsorption. Similar observations have been reported by other workers for adsorption of dyes indicating that the adsorbent has a net positive charge

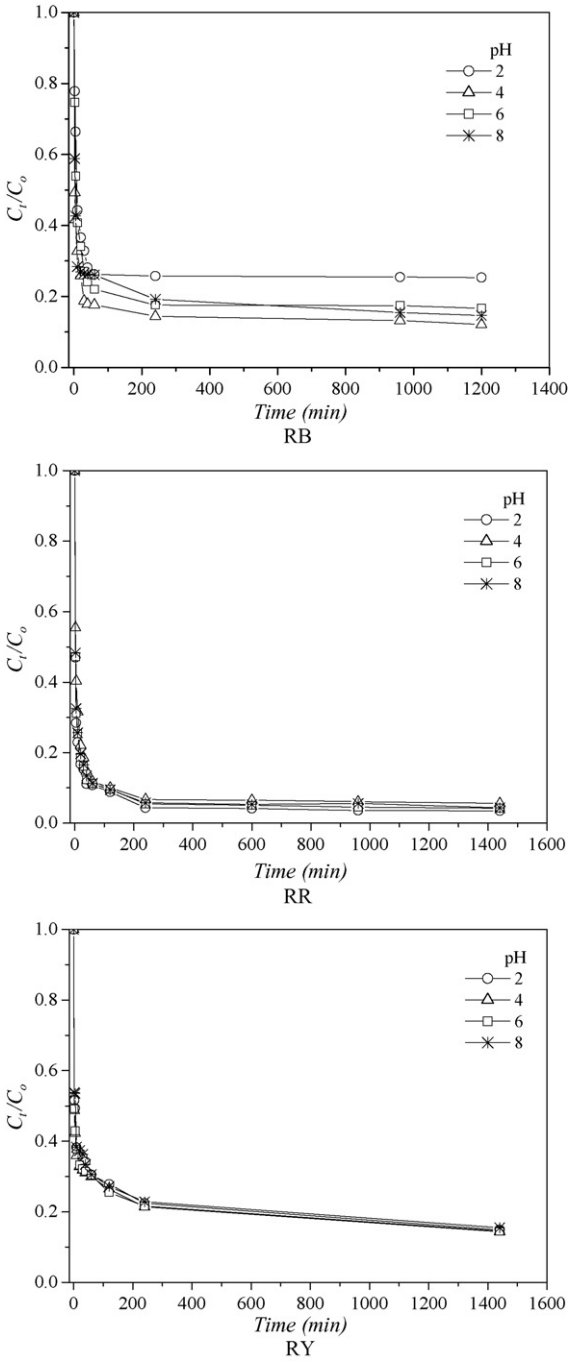

Fig. 5. Concentration–time profiles of RB, RR and RY reactive dyes on FA at different pHs. Conditions: C_0: 100 mg/l, 0.6 g/100 ml adsorbent dose, 293 K, 45 μm particle size, 250 rpm.

on its surface [24] and this would attract the negatively charged functional groups located on the dye.

The kinetics of the reactive dyes adsorption on FA is treated with diffusion controlled kinetic models. Higher values of k_{id} illustrate an enhancement in the rate of adsorption (Table 2). The conformity between experimental data and the model-predicted values was expressed by the correlation coefficients (r^2). A relatively high r^2 value indicates that the model successfully describes the kinetics of reactive dye adsorption. Kinetic parameters such as the diffusion coefficients (external and internal

Table 2
Kinetic parameters for adsorption of RB, RR and RY reactive dyes on FA; pH

Dye	pH	k_{id} (mg/g min$^{1/2}$)	r^2	k_f (cm/s) × 10^5	r^2	D (cm^2/s) × 10^8	r^2
RB	2	0.374	0.997	1.276	0.997	2.263	0.989
	4	0.728	0.994	1.839	0.992	5.140	0.974
	6	1.199	0.975	1.815	0.946	10.288	0.989
	8	0.739	0.874	2.263	0.985	14.146	0.933
RR	2	0.076	0.968	0.024	0.966	6.224	0.971
	4	0.080	0.952	0.025	0.969	6.430	0.987
	6	0.091	0.902	0.028	0.981	6.687	0.988
	8	0.095	0.917	0.596	0.973	7.356	0.986
RY	2	0.113	0.979	0.808	0.961	0.875	0.985
	4	0.119	0.998	0.937	0.978	0.926	0.999
	6	0.141	0.989	0.992	0.959	0.977	0.992
	8	0.143	0.959	1.150	0.903	0.957	0.971

diffusion coefficients), adsorption rates and Biot numbers are evaluated from Eqs. (2)–(6) and compiled in Table 2.

For the present systems, the values of the internal diffusion coefficient, D shown in Table 2, fall well within the magnitudes reported in literature [25], specifically for chemisorption systems (10^{-5} to 10^{-13} cm^2/s). The corresponding diffusion coefficients for the various concentrations of the reactive dyes varied from 2.26×10^{-8} to 14.15×10^{-8} cm^2/s for RB, 6.22×10^{-8} to 7.36×10^{-8} cm^2/s for RR and 0.88×10^{-8} to 0.96×10^{-8} cm^2/s for RY reactive dyes, respectively. The increase in D values is attributed to the increase in the internal surface affinity [26]. The Biot number obtained in the present study are higher than 100 indicating that the intraparticle diffusion is rate determining step since external diffusion has no physical significance for the reactive dye adsorptions onto FA.

4.5. Effect of initial concentration on adsorption kinetics

The effects of initial RB, RR and RY reactive dye concentrations on the rate of adsorption are shown in Fig. 6 as a plot of dimensionless concentration versus time for dye concentrations ranging from 100 to 500 mg/l. It is evident from figure that the amount adsorbed increases approximately from 73 to 235 mg/g for RY, from 52 to 165 mg/g for RB and from 56 to 135 mg/g for RR reactive dyes, respectively, when the initial concentration changed from 100 to 500 mg/l (Fig. 6). It is clear that the removals of the dyes were dependent on the concentration of the dyes. The rate of adsorption decreased with time until it gradually approached a plateau due to the continuous decrease in the concentration driving force. Moreover, the initial rate of adsorption was greater for higher initial dye concentration since the resistance to the dye uptake decreased as the mass transfer driving force increased.

The adsorption data for q_t versus $t^{1/2}$ for the reactive dyes is shown in two stages (Fig. 7). The first straight portion depicts macropore diffusion and the second representing micropore diffusion [27]. These show only the pore diffusion data. Extrapolation of the linear portions of the plots back to the y-axis gives the intercepts, which provide the measure of the boundary layer thickness. The initial period is attributed to boundary layer diffusion effects or external mass transfer effects. The kinetic parameters calculated from the diffusion kinetic models are listed in Table 3. It was found that the intraparticle diffusion coefficients, k_{id}, and mass transfer coefficient, k_f, increased with the increasing of the initial dye concentration. The diffusion coefficients inside the particle pores, D, also increased in the same concentration range. This behavior of concentration dependent diffusivity agrees with literature works [27].

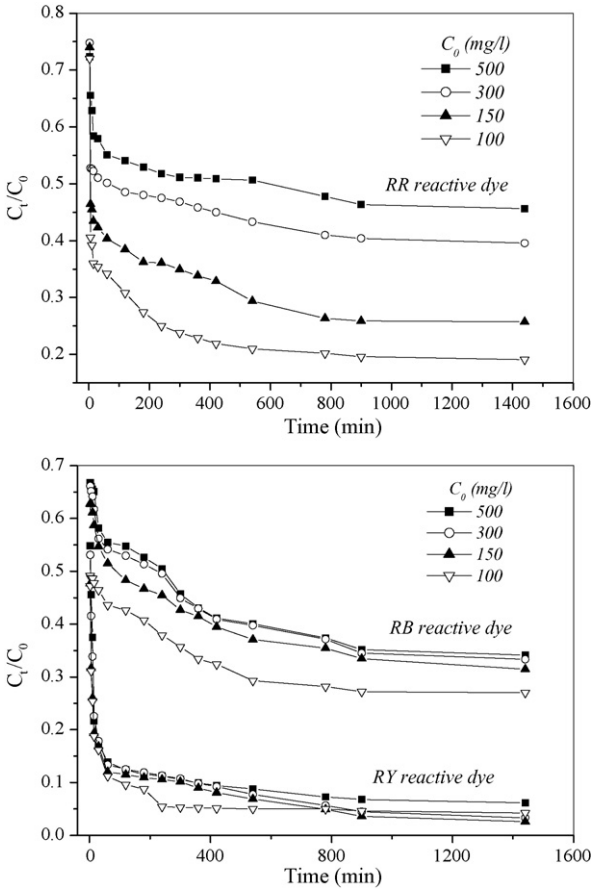

Fig. 6. Concentration–time profiles of RB, RR and RY reactive dyes on fly ash at different initial dye concentrations. Conditions: 0.6 g/100 ml adsorbent dose, 293 K, 45 μm particle size, pH 6, 250 rpm.

Table 3
Kinetic parameters for adsorption of RB, RR and RY reactive dyes on FA; C_0

Dye	C_0 (mg/l)	k_{id} (mg/g min$^{1/2}$)	r^2	k_f (cm/s) × 10^5	r^2	D (cm^2/s) × 10^8	r^2
RB	100	0.108	0.983	0.023	0.961	0.383	0.975
	150	0.127	0.992	0.060	0.952	0.419	0.921
	300	0.245	0.946	0.072	0.927	0.462	0.960
	500	0.374	0.975	1.839	0.946	0.514	0.989
RR	100	0.037	0.958	0.603	0.981	0.419	0.982
	150	0.058	0.966	1.467	0.927	0.431	0.974
	300	0.119	0.984	1.543	0.979	0.566	0.964
	500	0.178	0.963	1.689	0.954	0.687	0.988
RY	100	0.119	0.989	0.808	0.981	0.535	0.961
	150	0.179	0.956	0.140	0.951	0.567	0.955
	300	0.362	0.964	0.143	0.991	0.617	0.945
	500	0.636	0.970	0.154	0.978	0.926	0.992

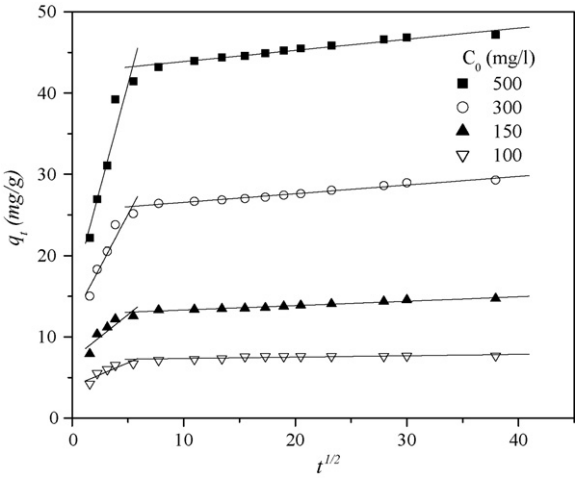

Fig. 7. The adsorption data for q_t vs. $t^{1/2}$ for RR reactive dye on FA at different initial concentrations. Conditions: 0.6 g/100 ml adsorbent dose, 293 K, 45 μm particle size, pH 6, 250 rpm.

The corresponding diffusion coefficients of the reactive dyes for 100–500 mg/l concentration range varied from 3.83×10^{-9} to 5.14×10^{-9} cm^2/s for RB, 4.19×10^{-9} to 6.87×10^{-9} cm^2/s for RR and 5.35×10^{-9} to 9.26×10^{-9} cm^2/s for RY reactive dyes, respectively. Hence, the concentration of reactive dye in the solution had a strong influence on both the adsorption diffusion kinetics and the mechanism controlling the kinetic coefficient.

5. Adsorption isotherms

The equilibrium adsorption isotherm is of importance in the design of adsorption systems. Several adsorption isotherm equations are available and the two important isotherms are selected in this study, the Langmuir and Freundlich isotherms [28,29].

The Langmuir isotherm assumes that sorption takes place at specific homogeneous sites within the adsorbent and has been successfully applied to many sorption processes. The linear form of Langmuir isotherm is given by the following equation:

$$\frac{C_e}{q_e} = \frac{1}{Q_0 b} + \frac{C_e}{Q_0} \quad (7)$$

where C_e is the equilibrium concentration (mg/l), q_e the amount adsorbed at equilibrium (mg/g), Q_0 the adsorption capacity (mg/g) and b is the energy of adsorption (Langmuir constant, l/mg). The values of Q_0 and b were calculated from the slope and intercept of the linear plots C_e/q_e versus C_e which gives a straight line of slope $1/Q_0$ which corresponds to complete monolayer coverage (mg/g) and the intercept is $1/Q_0 b$ (plots not shown).

The Freundlich isotherm describes equilibrium on heterogeneous surfaces and hence does not assume monolayer capacity. The isotherm is described by the following equations:

$$q_e = k_F C^{1/n} \quad (8)$$

The logarithmic form of the equation becomes

$$\log(q_e) = \log k_F + \frac{1}{n} \log(C_e) \quad (9)$$

where k_F and n are Freundlich constants and were calculated from the slope and intercept of the Freundlich plots. It has been shown that n values between 1 and 10 represent good adsorption potential of the adsorbent. The values of Langmuir and Freundlich constants at different temperatures are shown in Table 4. The experimental data fit well with both adsorption isotherm models since the values of correlation coefficients (r^2) are close to 1 (Table 4). The increase in adsorption capacity of FA at higher temperature may be attributed to the enlargement of pore size or activation of the adsorbent surface. The calculated adsorption capacities with three FA particle sizes are given in Table 5 for three reactive dyes. As seen in Table 5, the adsorption capacity for the reactive dyes increased with the decrease in the particle diameter. At a particle size range of 45–112.5 μm the values of saturation capacities are 89–106, 48.8–54.6 and 22.5–33.3 mg/g for RB, RR and RY reactive dyes, respectively. The increase in capacity with decreasing particle size range mainly suggests that reactive dyes did not seem to penetrate the whole particle but instead adsorb near or on the FA surface [30].

5.1. Effect of adsorbent particle size

The influence of adsorbent particle size was studied using RB, RR and RY reactive dyes on FA. Fig. 8 shows the experi-

Table 4
Parameters of Langmuir and Freundlich isotherms for RB, RR and RY reactive dyes on FA at different temperatures

Reactive dye	Parameters T (K)	Langmuir isotherm			Freundlich isotherm		
		Q_0 (mg/g)	b (l/mg)	r^2	k_f (mg/g)	n	r^2
RB	293	135.69	0.1421	0.996	15.54	1.77	0.967
	303	157.98	0.1734	0.999	20.11	1.82	0.948
	313	168.07	0.2456	0.999	26.68	1.99	0.944
	323	179.64	0.3130	0.999	34.22	2.04	0.944
RR	293	47.26	0.1280	0.989	1.965	2.04	0.989
	303	58.86	0.1210	0.970	2.758	2.03	0.970
	313	73.53	0.1320	0.993	3.119	2.15	0.993
	323	87.41	0.1160	0.998	3.672	2.29	0.976
RY	293	37.26	0.2540	0.974	4.82	3.12	0.974
	303	45.27	0.2421	0.991	7.29	3.53	0.991
	313	53.82	0.2430	0.993	8.76	3.57	0.993
	323	61.24	0.2436	0.992	10.22	3.62	0.991

mental results obtained from a series of experiments performed using different particle sizes of FA. For a particle size range of 45–112.5 μm, the values of adsorption capacities decreased from 74.4 to 55.4 mg/g for RB, 45.6 to 36.6 mg/g for RR and 30.2 to 21.0 mg/g, respectively (Fig. 8). The adsorption capacities for the reactive dyes increased with the decrease in the particle size because the higher adsorption with smaller adsorbate particle may be attributed to the fact that smaller particles give large surface areas. Moreover, the inability of the large dye molecule might penetrate all the initial pore structure of FA. A similar phenomenon was also reported previously for the adsorption of certain dyes [31,32] in the literature.

5.2. Effect of temperature

The effect of temperature on adsorption of three reactive dyes was studied in the temperature range 293–323 K, and the results were shown for RR reactive dye as an example in Fig. 9. It was observed from the figure that the adsorption capacity of RR reactive dye increased from 42.4 to 80.1 mg/g due to the enlargement of the pore sizes of adsorbent particles at elevated temperatures. Similar trends are also observed by other researchers for liquid-phase adsorption [33]. This increase in adsorption with a rise in temperature can be explained on the basis of thermodynamic parameters such as change in free energy (ΔG°), enthalpy (ΔH°) and entropy (ΔS°) were calculated using the following equations:

$$(\Delta G^\circ) = -RT\ \ln(K_c) \tag{10}$$

$$\log K_c = \frac{\Delta S^\circ}{2.303R} - \frac{\Delta H^\circ}{2.303RT} \tag{11}$$

where K_c, R and T are the equilibrium constant of the adsorption process, gas constant and absolute temperature, respectively. ΔH° and ΔS° were calculated from the slope and intercept of van't Hoff plots of $\ln K_c$ versus $1/T$ (plots not shown). The thermodynamic parameters for the adsorption of RB, RR and RY reactive dyes in aqueous solutions on FA are at various temperatures summarized in Table 6. The calculated ΔH° values for RB, RR and RY are 28.85, 13.93 and 13.29 kJ/mol, respectively. The positive value of ΔH° indicates that the process is endothermic in nature. The negative values of ΔG° showed the spontaneous adsorption of reactive dyes on the adsorbent and the positive values of ΔS° suggest that the increased randomness at the solid-solution interface during the adsorption of reactive dyes in aqueous solution on FA. The adsorbed solvent molecules

Table 5
Parameters of Langmuir and Freundlich isotherms for RB, RR and RY reactive dyes on FA at different particle sizes at 293 K

Dye	d_p (μm)	Langmuir isotherm			Freundlich isotherm		
		Q_0 (mg/g)	b (l/mg)	r^2	k_f (mg/g)	n	r^2
RB	45.0	106.16	0.0016	0.996	8.02	1.62	0.973
	71.5	90.99	0.0024	0.987	6.43	1.59	0.970
	112.5	89.21	0.0033	0.973	4.31	1.41	0.968
RR	45.0	54.56	0.0509	0.969	2.47	2.20	0.954
	71.5	50.14	0.0778	0.968	1.25	1.81	0.949
	112.5	48.80	0.1161	0.961	1.89	1.47	0.956
RY	45.0	32.30	0.0326	0.993	3.69	3.12	0.984
	71.5	29.85	0.0533	0.987	3.23	2.75	0.987
	112.5	22.53	0.0773	0.994	3.17	2.73	0.983

Table 6
Thermodynamic parameters for the adsorption of RB, RR and RY reactive dyes on FA at different temperatures

Dye	Temperature (K)	$-\Delta G$ (kJ/mol)	ΔH (kJ/mol)	ΔS (kJ/K mol)	r^2
RB	293	7.21	28.85	0.122	0.999
	303	8.34			
	313	9.68			
	323	10.82			
RR	293	4.39	13.93	0.063	0.961
	303	4.95			
	313	5.92			
	323	6.18			
RY	293	5.48	13.29	0.064	0.956
	303	6.03			
	313	6.69			
	323	7.26			

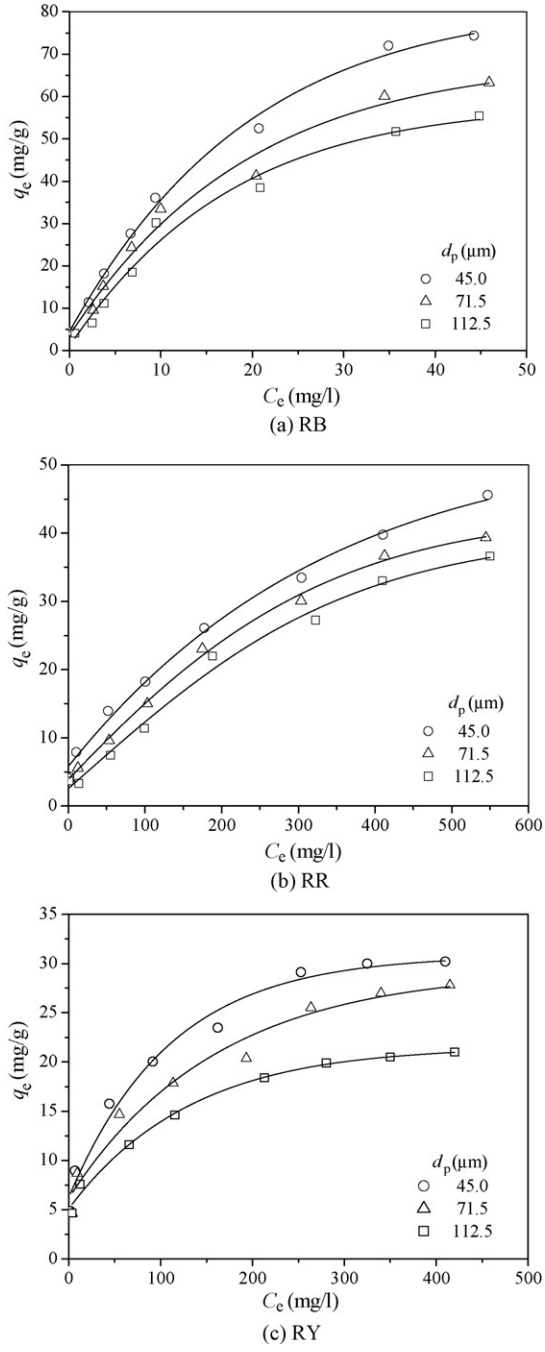

Fig. 8. Adsorption isotherms for (a) RB, (b) RR and (c) RY reactive dyes on FA at various particle sizes. Conditions: C_0: 50–1500 mg/l, 0.6 g/100 ml adsorbent dose, 293 K, pH 6, 250 rpm.

which are displaced by the adsorbate species gain more translational entropy than is ions lost by adsorbate thus allowing for prevalence of randomness in the system.

5.3. Comparison of adsorbents

A comparative evaluation of the adsorbent capacities of various types of adsorbents for the adsorption of reactive dyes is listed in Table 7. The adsorption capacities of the adsorbents used

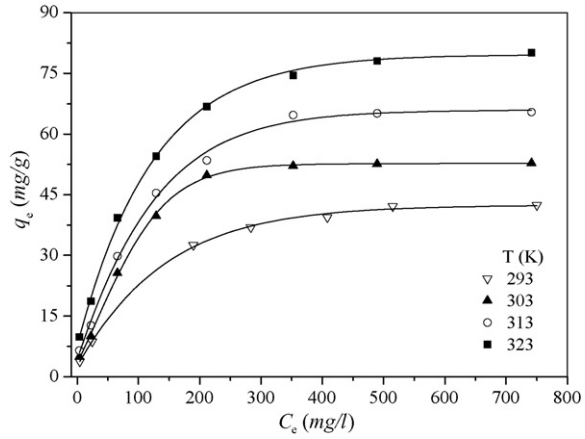

Fig. 9. Effect of temperature on the adsorption of RR reactive dye onto FA. Conditions: C_0: 50–1500 mg/l, 0.6 g/100 ml, 293 K, 45 μm particle size, pH 6, 250 rpm.

Table 7
Maximum adsorption capacity of various reactive dyes by some adsorbents

Adsorbent	Adsorbate	Adsorption capacity (mg/g)	Refs.
Baggase fly ash	Malachite Green	170.33	[34]
Fly ash	Reactive Blue	135.69	This study
Bagasse fly ash	Brillant Green	133.33	[38]
Fly ash (CFA)	Egacid Orange II	106.94	[11]
Coal fly ash	Methylene Blue	53.84	[39]
Fly ash	Reactive Red	47.26	This study
Coal fly ash	Crystal Violet	39.82	[14]
Fly ash	Reactive Yellow	37.26	This study
Bagasse fly ash	Methyl Violet	26.25	[35]
Bagasse fly ash	Orange-G	18.79	[35]
Baggase fly ash	Congo Red	11.88	[37]
Fly ash	Methylene Blue	8.23	[36]
Fly ash	Methylene Blue	7.55	[40]
Fly ash (CFA)	Methylene Blue	7.07	[11]
Fly ash (CFA)	Rhodamine B	5.51	[11]
Coal fly ash	Rosaline Hydrochloride	4.56	[14]
Fly ash	Acid Blue 9	4.31	[5]
Fly ash	Acid Red 91	1.46	[5]

in this study were not among the highest available but a relatively high uptake capacity of the dye could be obtained which makes the adsorbents suitable for colors removal in textile industry.

6. Conclusions

These experimental studies have indicated that FA has the potential to act as an adsorbent for the removal of RB, RR and RY reactive dyes from aqueous solutions. The effects of initial dye concentration and pH on the reactive dye removal were determined with the experimental data mathematically described using intraparticle and external mass transfer diffusion models. The experimental data showed conformity with an adsorption process, with the removal rate dependent on both intraparticle and external mass transfer diffusion. The adsorption data correlated well with Langmuir and Freundlich adsorption isotherm models. The adsorption of the reactive dyes increased with

increasing of initial dye concentration and temperature while decreasing with the particle size. Thermodynamical parameters were evaluated for three reactive dyes and revealed that the adsorption of the dyes is endothermic in nature. The positive value of ΔH° shows that adsorption is favorable at higher temperature and the presence of possible chemisorption phenomenon.

References

[1] H. Zollinger, Colour Chemistry-Synthesis, Properties and Application of Organic Dyes and Pigments, VCH, NewYork, 1987.

[2] E.A. Clarke, R. Anliker, Organic dye and pigments Handbook of Environmental Chemistry, Anthropogenic Compounds, Part A, vol. 3, Springer, New York, 1980.

[3] Y.M. Slokar, A.M. Le Marechal, Methods of decoloration of textile wastewaters, Dyes Pig. 37 (1997) 335–356.

[4] C. O'Neill, F.R. Hawkes, D.L. Hawkes, N. Lourenco, H.M. Pinheiro, W. Delee, Colour in textile effluents—sources, measurement, discharge consents and simulation: a review, J. Chem Technol. Biotechnol. 74 (1999) 1009–1018.

[5] K.R. Ramakrishna, T. Viraraghavan, Dye removal using low cost adsorbents, Water Sci. Technol. 36 (1997) 189–196.

[6] C. Namasivayam, R. Radhika, S. Suba, Uptake of dyes by a promising locally available agricultural solid waste: coir pith, Waste Manage. 21 (2001) 381–387.

[7] S.D. Khattri, M.K. Singh, Colour removal from dye wastewater using sugar cane dust as an adsorbent, Adsorpt. Sci. Technol. 17 (1999) 269–282.

[8] P.K. Malik, Dye removal from wastewater using activated carbon developed from sawdust: adsorption equilibrium and kinetics, J. Hazard. Mater. 113 (2004) 81–88.

[9] K. Kadirvelu, M. Palanival, R. Kalpana, S. Rajeswari, Activated carbon from an agricultural by-product, for the treatment of dyeing industry wastewater, Biores. Technol. 74 (2000) 263–265.

[10] K.V. Kumar, V. Ramamurthi, S. Sivanesan, Modeling the mechanism involved during the sorption of methylene blue onto fly ash, J. Colloid Interface Sci. 284 (2005) 14–21.

[11] P. Janos, H. Buchtova, M. Ryznarova, Sorption of dyes from aqueous solutions onto fly ash, Water Res. 37 (2003) 4938–4944.

[12] T. Viraraghavan, K.R. Ramakrishna, Fly ash for color removal from synthetic dye solutions, Water Qual. Res. J. Can. 34 (1999) 505–517.

[13] B. Acemioglu, Adsorption of Congo red from aqueous solution onto calcium-rich fly ash, J. Colloid Interface Sci. 274 (2004) 371–379.

[14] D. Mohan, K.P. Singh, G. Singh, K. Kumar, Removal of dyes from wastewater using fly ash, a low-cost adsorbent, Ind. Eng. Chem. Res. 41 (2002) 3688–3695.

[15] Z. Al-Qodah, Adsorption of dyes using shale oil ash, Water Res. 34 (2000) 4295–4303.

[16] M.L. Hall, W.R. Livingston, Fly ash quality, past, present and future, and the effect of ash on the development of novel products, J. Chem. Technol. Biotechnol. 77 (2002) 234–239.

[17] A. Findon, G. McKay, H.S. Blair, Transport studies for the sorption of copper ions by Chitosan, J. Environ. Sci. Health, A 28 (1993) 173–185.

[18] S. Rengaraj, S.H. Moon, Kinetic of adsorption of Co(II) removal from water and wastewater by ion exchange resins, Water Res. 36 (2002) 1783–1793.

[19] Y.S. Ho, G. McKay, Sorption of dye from aqueous solution by peat, Chem. Eng. J. 70 (1998) 115–124.

[20] K. Urano, H. Tachikawa, Process development for removal and recovery of phosphorus from wastewater by a new adsorbent, Ind. Eng. Chem. Res. 30 (1991) 1897–1899.

[21] E. Guibal, C. Milot, J.M. Tobin, Metal–anion sorption by chitosan beads: equilibrium and kinetic studies, Ind. Eng. Chem. Res. 37 (1998) 1454–1463.

[22] O. Bayat, Characterisation of Turkish fly ashes, Fuel 77 (1998) 1059–1066.

[23] P.M. Silverstein, G.C. Bassler, T.C. Morrill, Spectrometric Identification of Organic Compounds, Wiley, New York, 1991.

[24] A. Bousher, X. Shen, R.G.J. Edyvean, Removal of coloured organic matter by adsorption onto low-cost waste materials, Water Res. 31 (1997) 2084–2092.

[25] D. Chazopoulos, A. Varma, R.L. Irvine, Activated carbon adsorption and desorption of toluene in the aqueous phase, AIChE J. 39 (1993) 2027–2041.

[26] M.A.M. Khraisheh, Y.S. Al-Degs, S.J. Allen, M.N. Ahmad, Elucidation of controlling steps of reactive dye adsorption on activated carbon, Ind. Eng. Chem. Res. 41 (2002) 1651–1657.

[27] H.M. Asfour, M.M. Nassar, O.A. Fadali, M.S. El-Geundi, Colour removal from textile effluents using hardwood saw dust as an adsorbent, J. Chem. Technol. Biotechnol. A 35 (1985) 28–35.

[28] I. Langmuir, Adsorption of gases on plain surfaces of glass mica platinum, J. Am. Chem. Soc. 40 (1918) 1361–1403.

[29] H.M.F. Freundlich, Over the adsorption in solution, J. Phys. Chem. 57 (1906) 385–471.

[30] R.S. Juang, R.L. Tseng, F.C. Wu, S.H. Lee, Adsorption behaviour of reactive dyes from aqueous solutions on chitosan, J. Chem. Technol. Biotechnol. 70 (1997) 391–399.

[31] G. McKay, M.S. Otterburn, J.A. Aga, Fuller's earth and fired clay as adsorbents for dyestuffs, Water Air Soil Pollut. 24 (1985) 307–322.

[32] G.S. Gupta, G. Prasad, K.K. Panday, V.N. Singh, Removal of chrome dye from dye aqueous solutions by fly ash, Water Air Soil Pollut. 37 (1988) 13–24.

[33] C. Namasivayam, R.T. Yamuna, Adsorption of chromium(VI) by a low-cost adsorbent: biogas residual slurry, Chemosphere 30 (1995) 561–578.

[34] I.D. Mall, V.C. Srivastava, N.K. Agarwal, I.M. Mishra, Adsorptive removal of malachite green dye from aqueous solution by bagasse fly ash and activated carbon-kinetic study and equilibrium isotherm analyses, Colloid Surf. A 264 (2005) 17–28.

[35] I.D. Mall, V.C. Srivastava, N.K. Agarwal, Removal of Orange-G and Methyl Violet dyes by adsorption onto bagasse fly ash-kinetic study and equilibrium isotherm analyses, Dyes Pig. 69 (2006) 210–223.

[36] S. Wang, Y. Boyjoo, A. Choueib, Z.H. Zhu, Removal of dyes from aqueous solution using fly ash and red mud, Water Res. 39 (2005) 129–138.

[37] I.D. Mall, V.C. Srivastava, N.K. Agarwal, I.M. Mishra, Removal of congo red from aqueous solution by bagasse fly ash and activated carbon: kinetic study and equilibrium isotherm analyses, Chemosphere 61 (2005) 492–501.

[38] V.S. Mane, I.D. Mall, V.C. Srivastava, Use of bagasse fly ash as an adsorbent for the removal of brilliant green dye from aqueous solution, Dyes Pig. 73 (2007) 269–278.

[39] T. Viraraghavan, K.R. Ramakrishna, Fly ash for colour removal from synthetic dye solutions, Water Qual. Res. J. Can. 34 (1999) 505–517.

[40] V.K. Gupta, D. Mohan, S. Sharma, M. Sharma, Removal of basic dyes (rhodamine B and methylene blue) from aqueous solutions using bagasse fly ash, Sep. Sci. Technol. 35 (2000) 2097–2113.